

THE INTERNATIONAL SOCIETY OF  
PRECISION AGRICULTURE PRESENTS THE  
13th INTERNATIONAL CONFERENCE ON  
**PRECISION AGRICULTURE**

July 31-August 4, 2016 • St. Louis, Missouri USA

## Creating prescription maps from historical imagery for site-specific management of cotton root rot

Chenghai Yang<sup>1</sup>, G. N. Odvody<sup>2</sup>, J. A. Thomasson<sup>3</sup>, T. Isakeit<sup>3</sup>, R. L. Nichols<sup>4</sup>

<sup>1</sup>USDA-ARS, Aerial Application Technology Research Unit, College Station, TX

<sup>2</sup>Texas AgriLife Research and Extension Center, Corpus Christi, TX;

<sup>3</sup>Texas A&M University, College Station, TX;

<sup>4</sup>Cotton Incorporated, Cary, NC

A paper from the Proceedings of the  
13<sup>th</sup> International Conference on Precision Agriculture  
July 31 – August 4, 2016  
St. Louis, Missouri, USA

**Abstract.** Cotton root rot, caused by the soilborne fungus *Phymatotrichopsis omnivore*, is a severe plant disease that has affected cotton production for over a century. Recent research found that a commercial fungicide, Topguard (flutriafol), was able to control this disease. As a result, Topguard Terra Fungicide, a new and more concentrated formulation developed specifically for this market was registered in 2015, so cotton producers can use this product to control the disease. Cotton root rot only infects isolated portions of the field and tends to occur in the same general areas within the field in recurring years. The unique characteristic of cotton root rot makes it an excellent candidate for site-specific management based on historical infection maps. Remote sensing in conjunction with image classification techniques has been successfully used to detect cotton root rot and create classification maps. Although these maps can be directly used as prescription maps for site-specific fungicide application, some practical issues need to be considered for creating prescription maps. Two of these issues include the accommodation of the variation or potential expansion of the disease over years and consideration of minimum areas that can be practically managed. Moreover, it is important to select an accurate and effective image classification method that can be easily implemented. The objective of this study was to develop practical procedures to create prescription maps from remotely sensed imagery for site-specific treatment of cotton root rot. Airborne multispectral imagery taken from a cotton field with a history of cotton root rot in south Texas in 2002 and 2012 was used to illustrate the process. The images were rectified and resampled to the same pixel size (1 m) between the two years. The normalized difference vegetation index (NDVI) images were generated and unsupervised classification was then used to classify the NDVI images into root

rot-infected and non-infected zones. Small inclusions of areas within the dominant zones were eliminated using different thresholds. Other artifacts such as missing plants due to planter skips and crop damage caused by wheel tracks of the center-pivot system were merged to the non-infected zone. Change detection analysis was performed to detect the consistency and change in root rot infection between the two growing seasons. To account for the potential expansion and temporal variation of the disease, buffer zones of 1-20 m around the infected areas were created and the effect of the buffers on treatment areas was analyzed. The selection of buffer distance and minimum management areas in the prescription maps was discussed. This study demonstrates the practical procedures and considerations for creating prescription maps from historical images. The results will provide cotton producers, consultants and service providers with practical guidelines for developing prescription maps for site-specific management of control cotton root rot.

**Keywords.** Airborne imagery, cotton root rot, site-specific fungicide treatment, image classification, change detection, prescription map.

---

The authors are solely responsible for the content of this paper, which is not a refereed publication. Citation of this work should state that it is from the Proceedings of the 13th International Conference on Precision Agriculture. EXAMPLE: Yang, C., Odvody, G. N., Thomasson, J. A., Isakeit, T., & Nichols, R. L. (2016). Creating prescription maps from historical imagery for site-specific management of cotton root rot. In Proceedings of the 13th International Conference on Precision Agriculture (unpaginated, online). Monticello, IL: International Society of Precision Agriculture.

---

## Introduction

Cotton root rot, caused by the soilborne fungus *Phymatotrichopsis omnivora*, is a destructive cotton disease occurring throughout the southwestern United States. The symptoms usually begin during extensive vegetative growth, are more visible during flowering and fruit development, and continue through the growing season (Smith et al., 1962). Plants infected earlier in the growing season will die before bearing fruit, whereas infection occurring at later growth stages will reduce cotton yield and lower lint quality (Ezekiel and Taubenhaus, 1934; Yang et al., 2005).

Cotton root rot has plagued the cotton industry for more than 100 years (Pammel, 1988; Uppalapati et al., 2010). Despite decades of research efforts, effective practices for control of this disease were lacking until Topguard® Fungicide, a commercial formulation of flutriafol from Cheminova, Inc. (Wayne, NJ), showed considerable promise for suppressing this disease in field studies (Isakeit et al., 2009, 2012). Topguard (flutriafol) was used effectively in Texas from 2012 to 2015 to control cotton root rot under Section 18 emergency exemptions granted by the U.S. Environmental Protection Agency (EPA). As a result, growers achieved lower cotton root rot incidence, higher yields, and better fiber quality (Drake et al., 2013). In early 2015, Topguard® Terra Fungicide, a new and more concentrated formulation of flutriafol developed specifically for this market, was registered by the EPA. It provides the same level of cotton root rot control as Topguard.

Growers currently treat their fields uniformly even though they are aware that only portions of their fields are infected. One of the reasons for the uniform treatment is that growers want to make sure all existing and potential new infections are treated since they are not sure if the infection patterns will expand from year to year. Another reason is that site-specific application equipment and the practical tools to create prescription maps are not readily available for their use. Therefore, it is necessary to define the infected areas within the field so that variable rate technology can be used to apply the fungicide only to the infected areas for more effective and economical control.

Remote sensing is perhaps the only practical means for accurately and effectively mapping this disease because of large numbers of infected areas and their irregular shapes within cotton fields. In our previous studies, airborne imagery has been successfully used to map the extent of cotton root rot infections near the end of the growing season when cotton root rot is fully pronounced for the season (Yang et al., 2005) and to monitor the progression of the infections within cotton fields during a growing season (Yang et al., 2014). In these studies, ISODATA (Iterative Self-Organizing Data Analysis) unsupervised classification applied to multispectral imagery has been used to identify root rot-infected areas. With this method, the optimal number of spectral classes is determined based on the average transformed divergence for each classification map. The spectral classes are then grouped into root rot-infected and non-infected zones.

More recently, Yang et al. (2015) evaluated and compared two unsupervised classification techniques (ISODATA applied to multispectral imagery and to NDVI) and six supervised classification techniques (minimum distance, Mahalanobis distance, maximum likelihood, spectral angle mapper (SAM), neural net, and support vector machine (SVM)) for mapping and detecting cotton root rot from airborne multispectral imagery. Although all eight techniques appear to be equally effective and accurate for mapping cotton root rot, the NDVI-based classification can be easily implemented without the need for complex image processing capability. Therefore, it has been recommended as one of the simple and accurate classification methods to map cotton root rot and develop prescription maps for effective and economical control of this disease.

The objectives of this study were to: 1) develop practical procedures to create prescription maps from remotely sensed imagery for site-specific treatment of cotton root rot; and 2) assess the feasibility to use historical imagery to create prescription maps for site-specific management of the disease.

## Materials and methods

### Aerial imagery acquisition

Aerial imagery taken over a 10-year interval from a 97-ha center-pivot irrigated field with center coordinates of (28° 1'10.86"N, 97°42'49.22"W) near Edroy, Texas was selected for this study. This field had a history of cotton root rot and aerial imagery was taken in 2002 and 2012 when cotton was planted to the field.

A different imaging system was used to acquire images from the field in each of the two years shortly before harvest when root rot was fully expressed for the respective season. A three-camera imaging system described by Escobar et al. (1997) was used to acquire imagery on 19 July 2002. The imaging system consisted of three digital charge coupled device (CCD) cameras and a computer equipped with three image digitizing boards that had the capability of obtaining 8-bit images with 1024 × 1024 pixels. The three cameras were filtered for spectral observations in the green (555–565 nm), red (625–635 nm), and near-infrared (NIR, 845–857 nm) wavelength intervals, respectively.

A two-camera imaging system described by Yang et al. (2014) was used to take imagery on 25 July 2012. The system consisted of two consumer-grade digital cameras with a 5616 × 3744 pixel array. One camera captured normal RGB color images, while the other camera was equipped with a 720-nm long-pass filter to obtain NIR images.

A Cessna 206 single-engine aircraft was used to acquire imagery from the field in both years at an altitude of 3050 m (10,000 ft) above ground level between 1130h and 1530h local time under sunny conditions. Images from the three-camera system were saved to an on-board computer as three-band Tiff files, while images from the two-camera system were stored in two separate CompactFlash (CF) cards in both 14-bit RAW and 8-bit JPEG files. The ground pixel size achieved was 1.3 m in 2002 and 1.0 m in 2012.

### Image processing and classification

One composite image from each year was selected for analysis. An image-to-image registration procedure based on the first-order polynomial transformation model was used to align the individual band images in the three-band composite image as well as the RGB and NIR images from the two-camera system. The aligned images were then georeferenced or rectified to the Universal Transverse Mercator (UTM), World Geodetic System 1984 (WGS-84), Zone 14, coordinate system based on a set of ground control points around the field located with a Trimble GPS Pathfinder ProXRS receiver (Trimble Navigation Limited, Sunnyvale, California). The root mean square errors for rectifying the images using first-order transformation were within 2 m. All images were resampled to 1 m resolution using the nearest neighborhood technique. All procedures for image alignment and rectification were performed using ERDAS Imagine (Intergraph Corporation, Madison, Alabama).

The rectified images for the two dates were stacked as one image and a field boundary or an area of interest (AOI) was defined for the field. Normalized difference vegetation index (NDVI) images were calculated using the formula  $NDVI = (NIR - Red) / (NIR + Red)$ , where NIR and RED stand for the reflectance values for the NIR and red bands, respectively.

The NDVI images were classified into root rot-infected and non-infected zones using ISODATA unsupervised classification (Intergraph Corporation, 2013). The ISODATA method began with two classes and arbitrary class means from the NDVI image statistics. Each pixel was assigned to the class that had a smaller NDVI difference to the pixel. Each time the clustering repeated, the means of the two classes were recalculated and used for the next iteration. The process continued until the number of iterations reached 100 or the percentage of unchanged pixels reached 99.99% between two iterations. Pixels with lower NDVI values correspond to the root rot-infected zone, while pixels with higher NDVI values belong to the non-infected zone.

## Classification map filtering

The classification maps contained a large number of small polygons that were as small as 1 m<sup>2</sup>. Some of the polygons were correctly classified, while others were not. Small inclusions of areas within the dominant zones were eliminated using a threshold of 5 m<sup>2</sup>, considering the smallest areas that could be practically managed. Other artifacts such as missing plants due to planter skips and crop damage caused by wheel tracks of the center-pivot system had similar spectral response to cotton root rot and were therefore merged to the non-infected zone. The classification maps generated in ERDAS Imagine were converted into polygons for filtering and merging operations using ArcInfo GIS (ESRI, Inc., Redlands, California).

## Change detection and buffer creation

Change detection analysis was performed on the classification maps to determine the class changes between the two years. Change detection statistics, including common root rot areas in both years and root rot areas only in one of the two years, were calculated.

To simulate the potential expansion and temporal variation of the disease, buffer zones around the infected areas were created using ArcInfo GIS. The filtered classification maps were used to create buffer zones of 1–20 m with an increment of 1 m around the infected areas. The total area of the original root rot areas and the buffered areas for each of the 20 buffer distances were derived from the buffered maps.

## Results and discussion

### Image classification

Fig. 1 shows the color-infrared (CIR) images acquired in 2002 and 2012 and the respective two-zone classification maps after the small polygons and artifacts were removed for the field. On the CIR images, non-infected plants showed a reddish-magenta tone, while infected plants had a greenish or cyanish color. The root rot-infected areas can be easily distinguished from the non-infected areas on the CIR images.

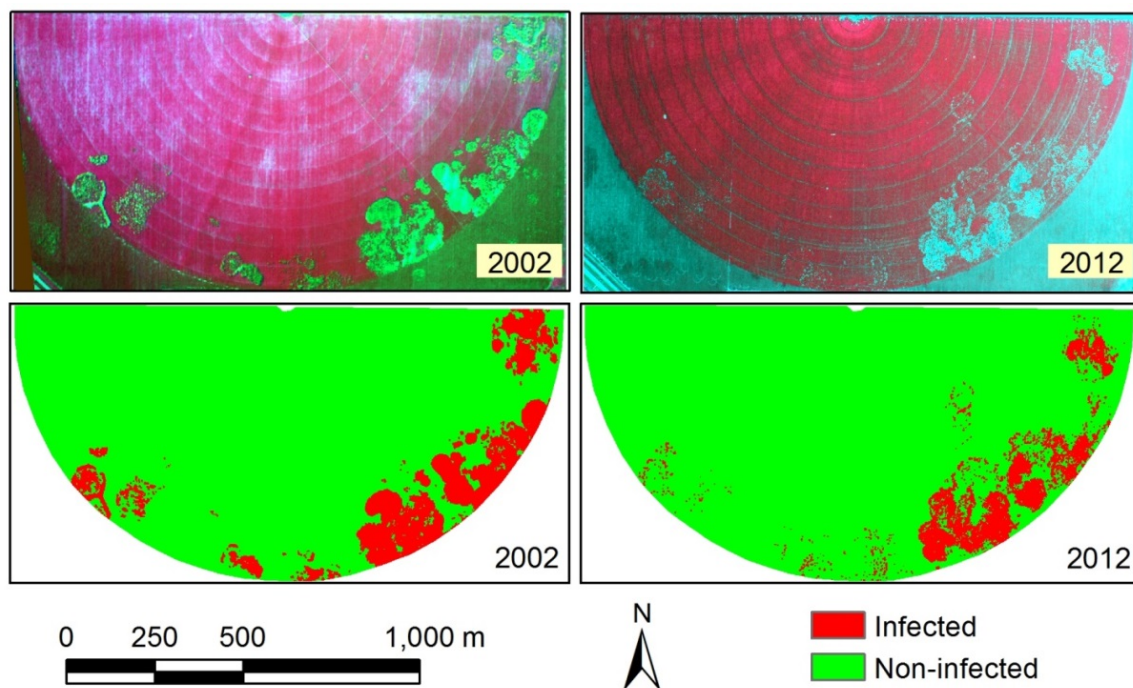


Fig. 1. Airborne color-infrared images (top) and two-zone classification maps (bottom) derived from NDVI images for a 97-ha cotton root rot-infected field near Edroy, Texas in 2002 and 2012.

A visual comparison of the classification maps and their respective CIR images indicates that the two-zone classification maps effectively identify apparent root rot areas within the field. The estimated percent root rot areas for the field were 11.7% in 2002 and 8.7% in 2012. The overall spatial patterns of infections between the two years were similar, but the infected area decreased in 2012 because some of the infected areas in 2002 were not fully pronounced in 2012. Nevertheless, cotton root rot occurred in the same general areas within the field and there were a few newly-infected areas in 2012.

### Change detection

Fig. 2 shows the overlaid map (left) of the two classification maps in 2001 and 2011 and the merged two-zone map for the field. In the overlaid map, the red shows the infected areas in both years, the blue shows the infected areas only in 2002, and the yellow depicts the infected areas only in 2012. Change detection analysis showed that 5.3% of the field was infected in both years, while 6.4% of the field was infected only in 2002 and 2.8% only in 2012 (Table 1). Thus, the total infected area in either 2002 or 2012 was 14.5% (5.3% + 6.4% + 2.8%) as shown by the merged two-zone map in Fig. 2 (right).

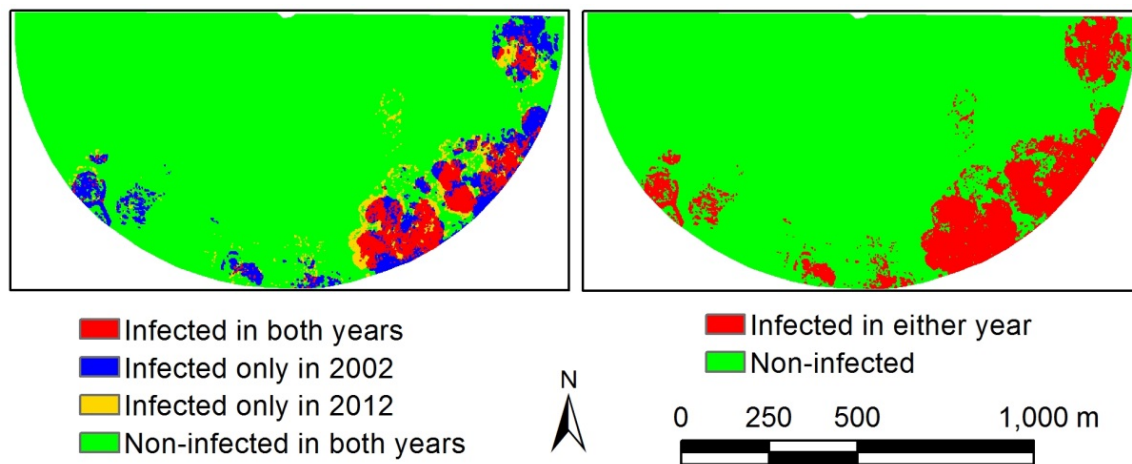


Fig. 2. Overlaid four-zone classification map between 2002 and 2012 (left) and merged two-zone classification map for a cotton root rot-infected field.

Table 1. Change detection statistics in terms of percent area (%) between two classification maps from airborne imagery acquired in 2002 and 2012 for a cotton root rot-infected field.

		Initial state (2002)			
		Class	Infected	Non-infected	Row total
Final state (2012)	Infected		5.3	2.8	8.1
	Non-infected		6.4	85.5	91.9
Column total			11.7	88.3	
Class change			-3.6	3.6	

### Effect of buffer distance on root rot maps

Fig. 3 presents the percent root rot areas with buffers of 0–20 m for the two separate years and the two years combined for the field. It can be seen clearly that percent area increased with buffer distance, but the increase rate decreased with buffer distance. At smaller buffer distances, percent area increased faster. At larger buffer distances, percent area increased at a slower rate. The reason for this difference is partly due to the fact that the original classification maps contained many small polygons and these polygons expanded in all directions and quickly filled the gaps between polygons at smaller buffer distances. As buffer distance increased further, the increase rate tended to reduce. Nevertheless, as buffer distance continues to increase, all three curves will eventually reach the 100% maximum.

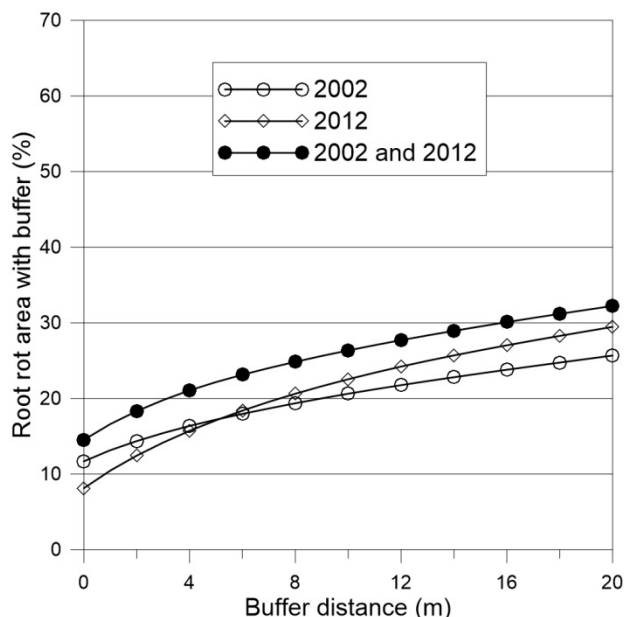


Fig. 3. Percent root rot area with buffers of 0–20 m for two separate years and the two years combined for a cotton root rot-infected field.

Table 3 summarizes the percent root rot area with buffer zones of 0–10 m around the infected areas for the separate years and the two years combined for the field. The percent root rot area increased from 11.7% for the 0-m buffer to 20.6% (1.8 times) for the 10-m buffer in 2002, and from 8.1% for the 0-m buffer to 22.6% (2.8 times) for the 10-m buffer in 2012. When the classification maps for the two years were merged, the percent root rot area increased from 14.5% for the 0-m buffer to 26.4% (1.8 times) for the 10-m buffer.

Table 2. Root rot area with buffer in percentage (%) at buffer distances of 0-11 m for 2002, 2012 and the two years combined for a cotton root rot-infected field.

Year	Buffer distance (m)										
	0	1	2	3	4	5	6	7	8	9	10
2002	11.7	13.1	14.4	15.4	16.4	17.2	18.0	18.7	19.4	20.0	20.6
2012	8.1	10.5	12.4	14.2	15.7	17.1	18.4	19.6	20.6	21.6	22.6
2002 & 2012	14.5	16.6	18.3	19.8	21.1	22.2	23.1	24.0	24.9	25.6	26.4

The expansion rate with buffer distance depends on the spatial distribution and extent of the original root rot infection. It can be seen from Fig. 3 and Table 3 that the expansion rate with buffer differed for different years. The expansion rate was much faster for 2012 than for 2002 due to newly-infected areas in 2012. Although original infection was smaller for 2012 than for 2002, the percent root rot area with a 5-m buffer for 2012 reached that for 2002.

Fig. 4 shows the two-zone classification maps with a 5-m buffer around infected areas for the two separate years and the two years combined for the field. The percent root rot areas with the buffer were 17.2%, 17.1% and 22.2% (or 1.5, 2.1 and 1.5 times the original infection) for 2002, 2012, and the two years combined. These maps along with other maps created with different buffer distances can be used for estimation of root rot areas and for site-specific fungicide application.

The selection of the optimal buffer distance depends on multiple factors such as infection extent and pattern, availability of imagery for single season or multiple seasons, and the producer's risk tolerance. For the example field used in this study, when the images from both years were used to create a merged classification map, a buffer distance of 5 m would be appropriate. When the image from one single year was used, a buffer distance of 10 m would be more appropriate. Table 2 shows the treatment areas and potential fungicide cost and savings for site-specific treatment of the field in this scenario. As the fungicide at full rate costs about \$124/ha (\$50/acre), it would cost \$12,000 to treat the 97-ha field uniformly. If only 22% of the field were treated, the fungicide cost would be about \$2,700 and the savings on reduced fungicide use would be over \$9,300 for the field. The savings

from reduced fungicide will far exceed the costs associated with the addition of a variable rate controller and the creation of prescription maps. Based on our aerial surveys, root rot-infected areas vary from 0 to 75% within fields, but most fields contain 20-40% infected areas. Therefore, there is a great potential for significant savings with site-specific treatment of cotton root rot.

**Table 2. Treatment areas and potential fungicide cost and savings for site-specific application for a cotton root rot-infected field.**

Year	Buffer distance (m)	Treatment area (ha)	Treatment area (%)	Fungicide cost at \$124/ha	Savings on fungicide
2002	10	20.0	20.6	\$2480	\$9548
2012	10	21.9	22.6	\$2716	\$9312
2002&2012	5	21.5	22.2	\$2666	\$9362

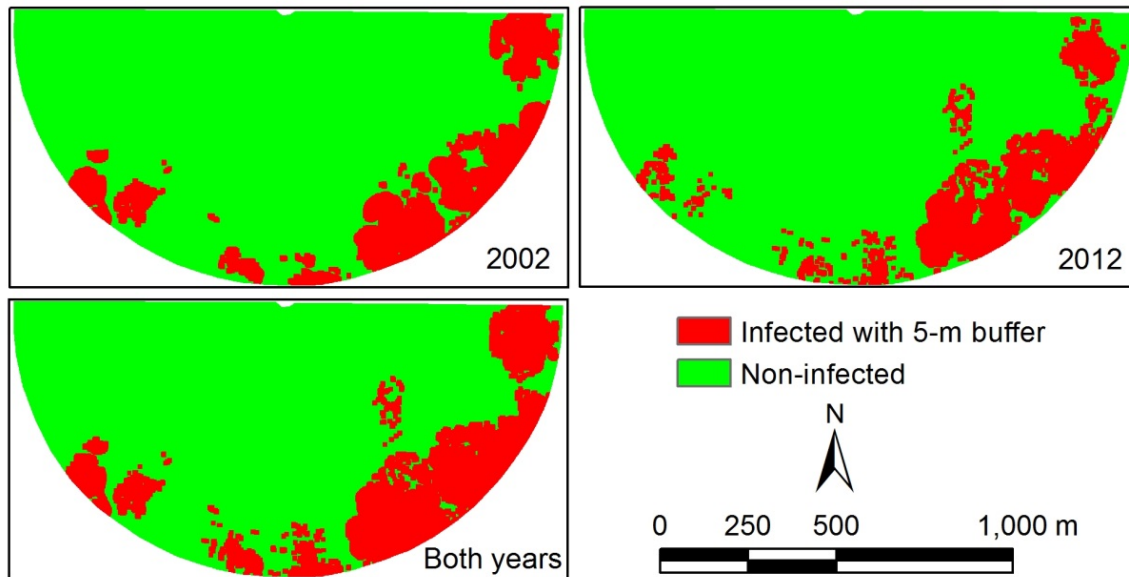


**Fig 4. Classification maps with a 5-m buffer around infected areas for 2002, 2012 and the two years combined for a cotton root rot-infected field.**

## Conclusions

Results from this study demonstrate that cotton root rot tends to occur in the same general areas within fields in recurring years, even though variations in infection patterns exist over the years. The relative stability of cotton root rot-infected areas indicates that historical remote sensing imagery can be used for the site-specific management of the disease in the future years. Numerous unsupervised and supervised image classification methods can be applied to multispectral imagery for accurately differentiating infected areas from non-infected areas, but the NDVI-based ISODATA classification appears to be a simple and effective method for generating root rot infection maps. To account for the potential expansion and temporal variation of the disease, buffer zones can be added around the infected areas in the original classification maps for generating prescription maps. The procedures and results presented in this paper provide general guidelines for the creation of prescription maps and have practical implications for site-specific management of cotton root rot.

## Acknowledgements

This project was partly funded by Cotton Incorporated at Cary, North Carolina. The authors wish to thank Rene Davis of USDA-ARS at Weslaco, Texas, Lee Denham and Fred Gomez of USDA-ARS at College Station, Texas for taking the imagery for this study. Thanks are also extended to John Barrett of Corpus Christi, Texas for allowing us to use his field. Mention of trade names or commercial products in this article is solely for the purpose of providing specific information and does not imply recommendation or endorsement by the U.S. Department of Agriculture. USDA is an equal opportunity provider and employer.

## References

- Drake, D. R., Minzenmayer, R. R., Multer, W. L., Isakeit, T., & Morgan, G. D. (2013). Evaluation of farmer applications of Topguard (flutriafol) for cotton root rot control in the first Section 18 exemption year. In Proceedings of Beltwide Cotton Conference (pp. 152–156). Memphis, TN: National Cotton Council of America.
- Escobar, D. E., Everitt, J. H., Noriega, J. R., Davis, M. R., & Cavazos, I. (1997). A true digital imaging system for remote sensing applications. In Proceedings of the 16th Biennial Workshop on Color Photography and Videography in Resource Assessment (pp. 470–484). Bethesda, MD: American Society for Photogrammetry and Remote Sensing.
- Ezekiel, W. N., & Taubenhaus, J. J. (1934). Cotton crop losses from *Phymatotrichum* root rot. *Journal of Agricultural Research*, 49(9), 843–858.
- Intergraph Corporation. (2013). *ERDAS Field Guide*. , Huntsville, AL: Intergraph Corporation.
- Isakeit, T., Minzenmayer, R. R., & Sansone, C. G. (2009). Flutriafol control of cotton root rot caused by *Phymatotrichopsis omnivora*. In Proceedings of Beltwide Cotton Conference (pp. 130–133). Memphis, TN: National Cotton Council of America.
- Isakeit, T., Minzenmayer, R. R., Drake, D. R., Morgan, G. D., Mott, D. A., Fromme, D. D., Multer, W. L., Jungman, M., & Abrameit, A. (2012). Fungicide management of cotton root rot (*Phymatotrichopsis omnivora*): 2011 results. In Proceedings of Beltwide Cotton Conference (pp. 235–238). Memphis, TN: National Cotton Council of America.
- Pammel, L. H. (1888). Root Rot of Cotton, or “Cotton blight”. *Texas Agric. Exp. Station Ann. Bull.* 4, 50-65.
- Smith, H. E., Elliot, F. C., & Bird, L. S. (1962). Root rot losses of cotton can be reduced. Pub. No. MP361. College Station, TX: Texas A&M Agricultural Extension Service.
- Uppalapati, S. R., Young, C. A., Marek, S. M., & Mysore, K. S. (2010). *Phymatotrichum* (cotton) root rot caused by *Phymatotrichopsis omnivora*: retrospects and prospects. *Molecular Plant Pathology*, 11(3), 325-334.
- Yang, C., Fernandez, C. J., & Everitt, J. H. (2005). Mapping *Phymatotrichum* root rot of cotton using airborne three-band digital imagery. *Transactions of the ASAE*, 48(4), 1619–1626.
- Yang, C., Odvody, G. N., Fernandez, C. J., Landivar, J. A., Minzenmayer, R. R., & Nichols, R. L. (2015). Evaluating unsupervised and supervised image classification methods for mapping cotton root rot. *Precision Agriculture*, 16, 201–215.
- Yang, C., Odvody, G. N., Fernandez, C. J., Landivar, J. A., Minzenmayer, R. R., Nichols, R. L., & Thomasson, J. A. (2014). Monitoring cotton root rot progression within a growing season using airborne multispectral imagery. *Journal of Cotton Science*, 18(1), 85-93.
- Yang, C., Westbrook, J. K., Suh, C. P., Martin, D. E., Hoffmann, W. C., Lan, Y., Fritz, B. K., & Goolsby, J. A. (2014). An airborne multispectral imaging system based on two consumer-grade cameras for agricultural remote sensing. *Remote Sensing*, 6, 5257–5278.